WARSAW UNIVERSITY OF TECHNOLOGY Index 351733
FACULTY OF CIVIL ENGINEERING
COMMITTEE FOR CIVIL AND WATER ENGINEERING
POLISH ACADEMY OF SCIENCES ISSN 1230-2945

DOI: 10.24425/ace.2022.143056

ARCHIVES OF CIVIL ENGINEERING

Vol. LXVIII ISSUE 4 2022

pp. 591 –606

Research paper

Optimal reshaping and stress controlling of double-layer spherical structures under vertical loadings

Ahmed Manguri[1,2], Najmadeen Saeed[3,4], Aram Mahmood[5], Javad Katebi[6], Robert Jankowski[7]

Abstract: Architectural structures' nodal coordinates are significant to shape appearance; vertical overloading causes displacement of the joints resulting in shape distortion. This research aims to reshape the distorted shape of a double-layer spherical numerical model under vertical loadings; meanwhile, the stress in members is kept within the elastic range. Furthermore, an algorithm is designed using the fmincon function to implement as few possible actuators as possible to alter the length of the most active bars. Fmincon function relies on four optimization algorithms: trust-region reflective, active set, Sequential quadratic progra mming (SQP), and interior-point. The fmincon function is subjected to the adjustment technique to search for the minimum number of actuators and optimum actuation. The algorithm excludes inactive actuators in several iterations. In this research, the 21st iteration gave optimum results, using 802 actuators and a total actuation of 1493 mm. MATLAB analyzes the structure before and after adjustment and finds the optimum actuator set. In addition, the optimal actuation found in MATLAB is applied to the modeled structure in MATLAB and SAP2000 to verify MATLAB results.

Keywords: optimization algorithms, spherical structures, double layers, shape and stress control, actuator

[1]MSc, PhD Student., Eng., Faculty of Civil and Environmental Engineering, Gdansk University of Technology, 80-223 Gdańsk, Poland, e-mail: ahmed.manguri@pg.edu.pl, ORCID: 0000-0002-3789-0006
[2]MSc, PhD Student., Civil Engineering Department, University of Raparin, Rania, Kurdistan Region, Iraq, e-mail: ahmed.manguri@uor.edu.krd, ORCID: 0000-0002-3789-0006
[3]Asst. Prof., PhD., Eng., Civil Engineering Department, University of Raparin, Rania, Kurdistan Region, Iraq, e-mail: najmadeen_qasre@uor.edu.krd, ORCID: 0000-0001-7074-0256
[4]Asst. Prof., PhD., Eng., Civil Engineering Department, Tishk International University, Erbil, Kurdistan Region, Iraq, e-mail: najmadeen.qasre@tiu.edu.iq, ORCID: 0000-0001-7074-0256
[5]MSc., Eng., Faculty of Civil Engineering University of Tabriz, Tabriz, Iran, e-mail: aram.osman22@gmail.com, ORCID: 0000-0001-9688-4311
[6]Asst.Prof., PhD., Eng., Faculty of Civil Engineering University of Tabriz, Tabriz, Iran, e-mail: jkatebi@tabrizu.ac.ir, ORCID: 0000-0002-6893-4526
[7]Prof., PhD., Eng., Eng Faculty of Civil and Environmental Engineering, Gdansk University of Technology, 80-223 Gdańsk, Poland, e-mail: jankowr@pg.edu.pl, ORCID: 0000-0002-6741-115X

1. Introduction

Spherical buildings are considered symbolic architectural structures. They are built as attraction buildings in tourist cities, such as Ericsson Globe in Stockholm, Sweden [1] and MSG Sphere in Las Vegas in the US [2]. Sometimes, the shape of such structures is distorted due to vertical overloading or unexpected loadings. This mainly happens when nodal joints are displaced due to external loadings. The outer face joints should be relocated to reshape the disturbing shape using adjustment techniques [3]. The idea of shape adjustment was introduced by Weeks [4], while its analytical procedure was given by Haftka and Adelman [5].

Since the coordinates of nodes define the geometry of structures, a slight change in their positions hugely affects the appearance of structures [6]. Controlling nodal positions can be done by changing some members' lengths with actuator devices [7]. Shape control of structures was performed utilizing various types of actors, namely thermal expansion [8], mechanical actuators [9], shape memory alloy (SMA) [10], and PZT actuators [11]. Mechanical actuators are presumed to be used in this study.

Researchers controlled the shapes of various structures, for example, spherical shell reflectors in space environments [12], cable mesh antennas [13, 14], and cable-stayed bridges [15]. Generally, during controlling structural shapes by changing the length of some members, the stress in some elements may reach a vulnerable range. To avoid such a situation, the designer should also observe the internal force of members [16, 17]. Some researchers focused only on stress without considering nodal displacements; for example, the axial force was controlled in prestressed cable domes [18] and cable net structures [19]. In some cases, it is essential to consider joint displacements and bar internal forces simultaneously, which is the case in this study. In terms of controlling shape and stress simultaneously, researchers used the bases of the Linear Force Method [20, 21]. In this study, the simultaneous equation previously introduced by Saeed and Kwan [3] is implemented to reshape the outer face of the numerical spherical model; meanwhile, the stress is kept within the yield stress limit.

Generally, providing many actuators and even large actuation may be costly. For the sake of the economy, it's reco mmended to use as few actuators as possible, which can be done by finding the optimum place for embedding actuators [16]. Furthermore, Joo et al. [22] conducted a study to find the optimum number of actuators to control morphing wing scissor mechanism configuration. In addition, Sabouni-Zawadzka and Zawadzki [23] presented a technique to find the most active cables to deploy a tensegrity model. In this study, the optimization techniques are subjected to adjustment equations to reduce the amount of actuation and minimize the number of actuators while the goals remain the same [17].

The optimization in this study relies on four algorithms: trust-region reflective, active set, SQP, and interior-point [24]. Heretofore optimal shape and stress control has been conducted for small-scale structures, such as cable structures [25–27] and truss structures [28]. Although it is essential to reshape and redistribute the stress of spatial systems available in the real world, only a few numbers of studies have been conducted on such structures.

Furthermore, measuring the stress and displacement of real structures is feasible, as stated by Liu et al. [29].

The form of architectural structures is significant [30]; therefore, it should be recovered when its shape is distorted due to loadings. The attempts to control shape and tress simultaneously for spatial structures were made for single-layer egg-shaped structures [31] and double-layer domes [32, 33]. Regarding the spherical structures, studies have not been conducted to reshape such architectural structures so far. In this research, the distorted shape of the exterior layer of the numerical spherical structure due to vertical loading is reshaped. Meanwhile, the stress in all members leashed within the yield stress domain. Furthermore, Optimization techniques are used to use as few as possible actuators and to optimize the amount of actuation.

A MATLAB program is used to analyze the structure before adjustment and to find the optimal actuator set. The actuation is applied to the modeled structure in MATLAB and SAP2000 to confirm the results. The outline of the papers is as follows: Section 1 presents background information about the techniques and structures that were previously adjusted. It is followed by Methodology. Section 3 shows the results in detail and provides a discussion about the results. Finally, Section 4 gives the conclusion of the work by providing essential outcomes.

2. Methodology

This section presents the techniques and software used in this research. In addition, structural geometry, properties of the materials, and the loading case are defined.

2.1. The adjustment technique

The Force Method [34] in MATLAB and Sap2000 is used to obtain the nodal displacements and the internal force of members. Now the target is set, which is the nullification of the displacement of the exterior face joints. The displacement adjustment equation is applied using MATLAB to receive the required actuation to accomplish the shape adjustment without regard to internal force. The equation has been presented by Saeed and Kwan [3].

$$\mathbf{Y}e_o + d_p = d_{tar} \tag{2.1}$$

where $\mathbf{Y}$ is the matrix formed by relating controlled nodes and actuators; while e_o is the actuation amount, d_p and d_{tar} are the nodal movements due to point loads and the prescribed displacement, respectively.

$$\mathbf{Z}e_o \leq t_p - t_{tar} \tag{2.2}$$

$\mathbf{Z}$ is formed by relating the targeted members and actuators. While t_p and t_{tar} are induced axial force due to external loads and prescribed internal bars force, correspondingly.

After applying e_o to the model, some members may face failure due to excessive stress. For this reason, Eq. (2.1) and (2.2) should be merged into Eq. (2.3) to control the displacement and stress simultaneously.

In the first step, only Eq. (2.1) has been implemented to see the necessity of improving the technique. When Eq. (2.1) is applied, stress passes the limit after applying the actuation to the members. Thus, the implementation of Eq. (2.3–2.4) is essential.

$$\begin{aligned} \mathbf{Y}e_o &= d_{tar} - d_p \\ \mathbf{Z}e_o &\leq t_p - t_{tar} \end{aligned} \tag{2.3}$$

$$\min f(x) = \sum_{i=1}^{n} e_{oi} \tag{2.4}$$

where n is the number of actuators, Eq. (2.4) is subjected to Eq. (2.3) to search for the minimum possible e_o using MATLAB. In other words, the conditions of the simultaneous equation is strictly preserved while the fmincon function searches for optimum actuators and optimal actuation. It should be noted that the algorithm works iteratively; the actuators with less than 0.1 mm are not considered in the next step since the value is insignificant and cannot be performed in practice.

2.2. Numerical model

The numerical model is modeled using MATLAB and SAP2000 software; the spherical structure consists of two layers; their center-to-center distance is 0.2 m. Furthermore, some extra members interconnect the two layers, resulting in increasing the degree of indeterminacy and enhancing the structure's stability. The number of outer and inner layer joints is 182 and 200, respectively, while the internal, exterior, and interconnection members are 420, 380, and 720, respectively. The detail of the joint and member numbering can be found in Fig. 1 and Table 1 respectively. Moreover, the 21 bottom joints are hinged supports that are restrained for the transition from all directions while the rotation of the members is permitted see Fig. 2.

Table 1. The details of the member numbering of the double layer spherical model

Members	From	To
Exterior circles	1	180
Interior circles	181	380
Connecting Exterior circles	381	580
Connecting interior circles	581	800
Connecting the exterior and interior circles	801	1520

```
Nr=20; Nc=11;  %Nr:is the number of base coordintes & Nc:is no. of circles
R=4000; Thick=200; %external reduis (mm) & distance between two layers(mm)
Layer=2; j=0;w=0; %Layer: no. of layers,
Th=0;Alpha=-90;%Th&Alpha: horizontal & vertical angle in degree
for Ly=1:Layer;
    for k=1:Nc-w;
        for i=1:Nr; j=j+1;
coor(j,1)= R*cosd(Alpha)*cosd(Th); coor(j,2)= R*cosd(Alpha)*sind(Th);
coor(j,3)= R*sind(Alpha);  Th=Th+360/Nr;
end;
Alpha=Alpha+180/(Nc-1);
    end;
    Th=360/(2*Nr); Alpha=-81;  w=w+1;R=R-Thick;
end;
jjj=coor
coor=coor([21:200,221:420,1, 201],:); %All coordinates
```

Fig. 1. A MATLAB code for joint coordinating

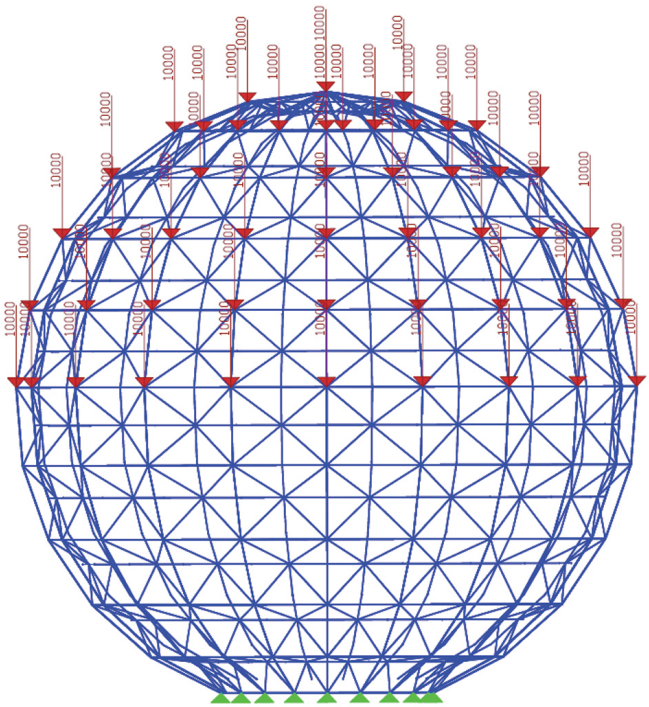

Fig. 2. The spherical double-layer numerical model under vertical point loadings

The outer and inner layers formed from 9 and 10 circles of joints on different levels. Each circle is shaped from 20 nodes at the same level as explained in Fig. 1. Except for the joints that shaped the circles, the coordinates of the very bottom and top joints (Joints 1 and 382) are (0, 0, –4000 and 0, 0, 4000) mm respectively.

The members' diameter is 10 mm with $E = 200$ GPa and $f_y = 720$ MPa, this type of steel material is called DP steel [35]. The internal force limit should be within the domain of $[-720 \cdot \frac{\pi}{4}10^2$ to $720 \cdot \frac{\pi}{4}10^2]$, equal to [–56549 to 56549] N. The allowable axial force of the members is calculated based on the Fy and crossectional area relationship $t = f_y \cdot A$.

The joints of the outer layer located above the midlevel (161 nodes) are loaded with 10 kN downward see Fig. 2; as a result, the model confronted a significant distortion, as shown in Fig. 3. In addition, it can be seen from Table 2 the Z-displacement values are more remarkable than that of the other directions. It should be highlighted that the nodal load is not removed even during and after adjustment.

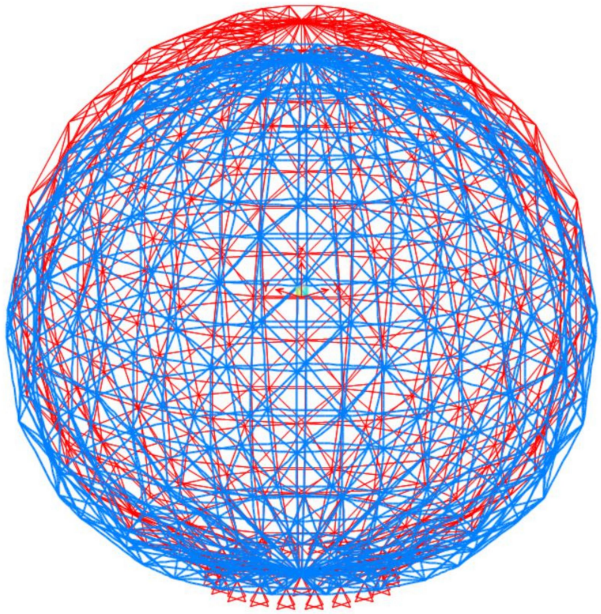

Fig. 3. Deformed shape of the spherical model after loading

2.3. MATLAB

The software analyzes the structure and implements optimization through fmincon function [36]. Furthermore, the program can be broadly advanced for problems in the structural engineering field. In this study, Eq. (2.3) is input in MATLAB as follows:

$$c_{eq} = [\mathbf{Y}e_o - d_d]$$
$$c = [-\mathbf{Z}e_o + tt_1,\ \mathbf{Z}e_o + tt_2]$$

The equality relationship (c_{eq}) should get value for e_o while the relationship $d_d = d_{tar} - d_p$ is preserved. Contrary, the inequality relationship searches for e_o that guarantees to keep the axial force in all members within the range [–56549 to 56549] N through $tt_1 = t_p - 56549$ and $tt_2 = t_p + 56549$.

2.4. SAP2000 program

SAP2000 is used to verify the analysis of the structure pre- and post-adjustment in MATLAB since SAP2000 cannot find actuation amounts for controlling nor performing optimization. The structure is modeled in the program and then analyzed to see if the results obtained in MATLAB before adjustment are correct. After applying Eqs. (2.3) and (2.4) in MATLAB, the obtained set of e_o is applied to the structure on MATLAB itself and SAP2000 to compare the results. SAP2000 program has a specific function that allows the user to insert force in the form of member's length altering. The function can be found under the Assign tab, frame load group, and Deformation function.

3. Results and discussion

The vertical loads inserted on the outer face joints, caused external nodal displacements resulting in shape distortion, as illustrated in Fig. 3. It was planned to reshape the exterior structural geometry, and all members were assumed to participate as actuators. Thus, Eq. (2.1) has been implemented to find the set of e_o. After applying the actuation to the members, the joint displacements of the outer layer of the spherical model were nullified. Although the nullification joint displacements were successful, the stress in some members [621 to 640] exceeds the yield stress. Therefore, while restoring the shape, the stress of members should be considered. Thus, the alternative to Eq. (2.1) is combining Eqs. (2.1) and (2.1) into Eq. (2.3).

Table 2 shows the nodal displacements of the outer face of the double layer model.

Table 2. Displacements of the outer layer joints Pre- and Post-adjustment

Joints*	Disp (mm)				Joints*	Disp (mm)			
	Pre-Adjustment			Post-Adjustment		Pre-Adjustment			Post-Adjustment
	MAT.&SAP.			MAT.&SAP.		MAT.&SAP.			MAT.&SAP.
	x	y	z	x, y & z		x	y	z	x, y & z
0–20	0	0	0	0	101	3.69	0	–28.32	0
21	4.89	0	–17.64	0	102,120	3.51	1.14	–28.32	0
22,40	4.65	1.51	–17.64	0	103,119	2.98	2.17	–28.32	0
23,39	3.95	2.87	–17.64	0	104,118	2.17	2.98	–28.32	0
24,38	2.87	3.95	–17.64	0	105,117	1.14	3.51	–28.32	0
25,37	1.51	4.65	–17.64	0	106,116	0	3.69	–28.32	0
26,36	0	4.89	–17.64	0	107,115	–1.14	3.51	–28.32	0
27,35	–1.51	4.65	–17.64	0	108,114	–2.17	2.98	–28.32	0
28,34	–2.87	3.95	–17.64	0	109,113	–2.98	2.17	–28.32	0
29,33	–3.95	2.87	–17.64	0	110,112	–3.51	1.14	–28.32	0
30,32	–4.65	1.51	–17.64	0	111	–3.69	0	–28.32	0
31	–4.89	0	–17.64	0	121	1.78	0	–30.5	0

Continued on next page

Table 2 – [cont.]

Joints*	Disp (mm)				Joints*	Disp (mm)			
	Pre-Adjustment			Post-Adjustment		Pre-Adjustment			Post-Adjustment
	MAT.&SAP.			MAT.&SAP.		MAT.&SAP.			MAT.&SAP.
	x	y	z	x, y & z		x	y	z	x, y & z
41	8.56	0	–23.32	0	122,140	1.7	0.55	–30.5	0
42,60	8.14	2.65	–23.32	0	123,139	1.44	1.05	–30.5	0
43,59	6.93	5.03	–23.32	0	124,138	1.05	1.44	–30.5	0
44,58	5.03	6.93	–23.32	0	125,137	0.55	1.7	–30.5	0
45,57	2.65	8.14	–23.32	0	126,136	0	1.78	–30.5	0
46,56	0	8.56	–23.32	0	127,135	–0.55	1.7	–30.5	0
47,55	–2.65	8.14	–23.32	0	128,134	–1.05	1.44	–30.5	0
48,54	–5.03	6.93	–23.32	0	129,133	–1.44	1.05	–30.5	0
49,53	–6.93	5.03	–23.32	0	130,132	–1.7	0.55	–30.5	0
50,52	–8.14	2.65	–23.32	0	131	–1.78	0	–30.5	0
51	–8.56	0	–23.32	0	141	–0.25	0	–33.59	0
61	7.02	0	–24.75	0	142,160	–0.24	–0.08	–33.59	0
62,80	6.68	2.17	–24.75	0	143,159	–0.2	–0.15	–33.59	0
63,79	5.68	4.13	–24.75	0	144,158	–0.15	–0.2	–33.59	0
64,78	4.13	5.68	–24.75	0	145,157	–0.08	–0.24	–33.59	0
65,77	2.17	6.68	–24.75	0	146,156	0	–0.25	–33.59	0
66,76	0	7.02	–24.75	0	147,155	0.08	–0.24	–33.59	0
67,75	–2.17	6.68	–24.75	0	148,154	0.15	–0.2	–33.59	0
68,74	–4.13	5.68	–24.75	0	149,153	0.2	–0.15	–33.59	0
69,73	–5.68	4.13	–24.75	0	150,152	0.24	–0.08	–33.59	0
70,72	–6.68	2.17	–24.75	0	151	0.25	0	–33.59	0
71	–7.02	0	–24.75	0	161	–0.88	0	–36.48	0
81	5.53	0	–26.53	0	162,180	–0.84	–0.27	–36.48	0
82,100	5.26	1.71	–26.53	0	163,179	–0.71	–0.52	–36.48	0
83,99	4.47	3.25	–26.53	0	164,178	–0.52	–0.71	–36.48	0
84,98	3.25	4.47	–26.53	0	165,177	–0.27	–0.84	–36.48	0
85,97	1.71	5.26	–26.53	0	166,176	0	–0.88	–36.48	0
86,96	0	5.53	–26.53	0	167,175	0.27	–0.84	–36.48	0
87,95	–1.71	5.26	–26.53	0	168,174	0.52	–0.71	–36.48	0
88,94	–3.25	4.47	–26.53	0	169,173	0.71	–0.52	–36.48	0
89,93	–4.47	3.25	–26.53	0	172	0.84	–0.27	–36.48	0
90,92	–5.26	1.71	–26.53	0	171	0.88	0	–36.48	0
91	–5.53	0	–26.53	0	382	0	0	–33.99	0

* y-direction sign conversion for the joints after the comma

The table shows only the joints that were targeted to be adjusted before and after applying e_o that obtained from Eq. (2.3). Firstly, when the structure was loaded with 10 kN downward to the outer layer joints, the load caused noticeable nodal displacements, the example of

some joint displacements tabulated in Table 2. The maximum external nodal displacement induced in the top joint is 36.48 mm. Furthermore, nullifying the nodal displacements of the outer layer and keeping the stress below 720 MPa in all members were the targets. It can be seen that the joints were relocated to their original coordinate after applying e_o (Table 2). Meanwhile, the internal force in all members kept below the yield stress level, as presented in Table 3. Table 3 clearly shows that none of the members surpassed the yield stress, though there were changes in the values of the stress of members before and after applying e_o.

To show only the critical members before and after adjustment (applying e_o), Table 3 shows only the number of members whose internal forces fall in the range of 40 to 56 kN either in tension or compression. The table shows that the compression members within 40 to 56 kN after adjustment are twice that before adjustment. The increasing stress in members after adjustment shows that the members were more affected by reshaping than stress redistribution. Furthermore, the number of tension and compression members of the whole structure before and after adjustment is illustrated in Fig. 4. The figure shows that the number of members in tension before adjustment was only 120 while the number markedly increased to 320. The reason could be shortening 39% of overall actuated members (Fig. 5).

Table 3. Members with larger than 40 kN internal force pre and post adjustment

Force (kN)		Pre-adjustment	Post-adjustment
Compression	56–55	625, 631, 632, 628, 629, 633, 635, 624, 637, 634, 639, 630, 636, 640, 627, 626, 638, 622, 623, 621	186, 181, 188, 187, 184, 198, 200, 195, 185, 191, 189, 629, 637, 630, 627,622, 625, 624, 628, 621, 635, 640, 626, 638, 636, 639, 623, 633, 632, 634, 631, 190, 197, 199, 183, 194, 192, 182, 196, 193
	50–54.9	–	–
	45–49.9	410, 409, 413, 407, 408, 412, 415, 405, 406, 414, 402, 411, 419, 404, 418, 416, 417, 401, 403, 420	365, 366, 367, 371, 364, 368, 380, 370, 369, 376, 372, 373, 377, 361, 375, 379, 374, 362, 378, 363
	40–44.9	–	417, 409, 406, 414, 419, 411, 416, 402, 405, 408, 413, 401, 420, 403, 407, 412, 410, 418, 404, 415
Tension	56–55	–	–
	50–54.9	238, 221, 229, 239, 226, 237, 228, 235, 236, 240, 222, 224, 227, 230, 223, 232, 234, 225, 233, 231	233, 221, 224, 234, 223, 228, 229, 225, 231, 227, 235, 240, 239, 232, 230, 238, 226, 236, 222, 237
	45–49.9	–	–
	40–44.9	43, 44, 46, 42, 48, 45, 50, 54, 47, 52, 60, 59, 51, 53, 55, 41, 57, 49, 56, 58	43, 44, 46, 42, 48, 45, 50, 54, 47, 52, 60, 59, 51, 53, 55, 41, 57, 49, 56, 58

The numbers tabulated in Table 3 have a descending order based on the value of the axial force. One can see that there are no members within the range 50–54.9 kN in compression before and after adjustment, similarly within the range 45–49.9 kN in tension. Numerically speaking, the internal force of Member 188 before adjustment was below

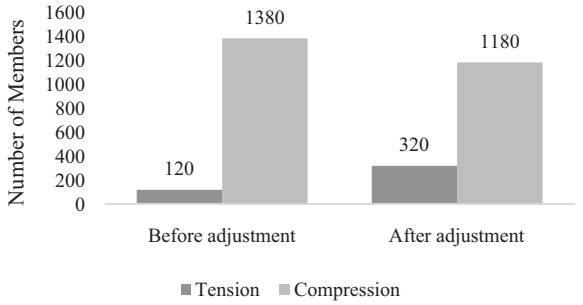

Fig. 4. The number of members in tension and compression pre and post adjustment

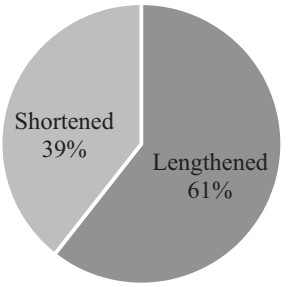

Fig. 5. The percentage of the shortened and lengthened of 802 members

40 kN, while the value dramatically rose to 56 kN. The reason could be that this member has been lengthened during adjustment.

Although Fig. 4 shows the number of members that faced compression was 1380 and 1180 before and after adjustment, Fig. 5 illustrates that most actuated members were lengthened. This is due to the fact the moved-down joints were moved up for reshaping. In other words most of the members were lengthened against the direction of loading, which causes significant compressive stress and keeps compression force as dominant as presented in Fig. 6.

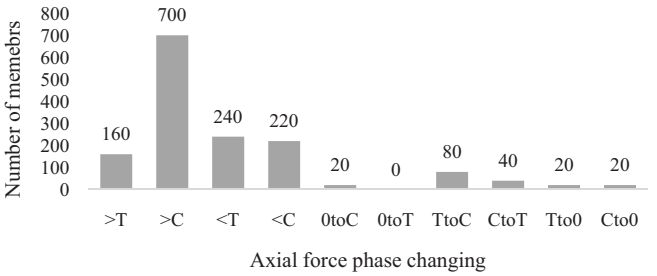

Fig. 6. Axial force phase changing in members after adjustment

Figure 5 illustrates that 61% of the actuated members are lengthened to achieve the goals; these members mainly are vertical ones. In contrast, the shortened members are horizontal ones, which helps bring up the dropped joints.

Figure 6 illustrates the changes in the number of members that changed their axial force value. First of all, it's clear all members (1500) changed their axial force values. One can see that 700 members increased their compressive stress since most of them were lengthened, as presented in Table 4. Furthermore, 80 members changed their phase from tension to compression, whereas half of that number changed the phase inversely. Moreover, 240 members reduced their tension force while 220 declined their compression force. In addition, 20 zero members faced compression while no zero members faced tension. Generally, compression force is dominant since the downward joints need to be moved up. Although compression force is vulnerable due to buckling, it was not considered in this study; it was assumed that the members have the same strength for tension and compression.

Table 4 shows each actuated member's actuation, while the values of e_o incremented to 0.5 mm. The left side covers the members that were shortened, while the right-hand side of the table presents the members that were lengthened. It can be clearly seen the majority of the members were lengthened. Moreover, in most cases, the lengthened members increased their compressive stress and vice versa. For example, Member 188 faced 326 N tension axial force before the adjustment; after extending it by 3.74 mm, the axial force turned to 56583 N compression. Contrary, members 43 to 49 had 41556 N before the adjustment; after shortening them by 2.63, 2.70, 2.49, 2.56, 2.55, 2.55, and 2.55, respectively, their tension force increased to 44685 N.

Table 4. Values of e_o of 802 active members

e_o (mm)	Members with negative e_o	Members with positive e_o
> 10	223	936, 906, 905
8–8.49	–	849
8.5–8.99	197	–
7.5–7.99	–	823, 934
7–7.49	197	672, 850
6.5–6.99	234, 222, 601, 274, 273, 229	629, 639, 679, 824
6–6.49	–	634
5.5–5.99	–	621, 640, 636, 626, 997, 1000
5–5.49	587, 987, 988	209, 622, 633, 667, 980
4.5–4.99	–	754, 581, 805, 866, 196, 628, 638, 198, 653
4–4.49	234, 222, 601, 274, 273, 229	607, 978, 414, 854, 647, 881, 882, 632, 865, 806, 625
3.5–3.99	230, 1455, 1456, 240, 186, 883, 227, 193	411, 756, 406, 412, 415, 403, 407, 409, 404, 417, 959, 402, 188, 960, 408, 410, 745, 419, 418, 654, 853, 401, 759, 413, 420, 416
3–3.49	238, 254, 260, 1156, 1127, 258, 1128, 624, 245, 233, 243, 1155, 875, 253, 251, 931, 257, 248, 256, 207, 247, 246	649, 940, 650, 651, 748, 627, 747, 814, 793, 405, 1135, 1136

Continued on next page

Table 4 – [cont.]

e_o (mm)	Members with negative e_o	Members with positive e_o
2.5–2.99	250, 252, 242, 975, 241, 660, 1475, 1476, 277, 249, 259, 948, 280, 255, 244, 44, 50, 1428, 55, 52, 264, 43, 54, 42, 871, 60, 57, 46, 47, 48, 59, 49, 56, 1463, 674	453, 741, 458, 589, 641, 942, 658, 642, 656, 941, 604, 652, 860, 840, 648, 456, 442, 187, 445, 666, 591, 744
2–2.49	275, 45, 298, 1419, 221, 51, 1420, 269, 288, 1427, 1107, 41, 276, 1108, 1464, 53, 228, 884, 231, 873, 239, 261, 285, 773, 58, 946, 270, 311, 295, 1415, 593, 263, 294, 204, 973, 1416, 300, 203, 299, 290, 262, 303, 208, 293, 296, 281, 287, 432	467, 485, 668, 487, 482, 630, 836, 497, 488, 481, 511, 677, 839, 500, 645, 495, 468, 475, 452, 498, 455, 472, 750, 194, 876, 659, 833, 441, 657, 635, 479, 460, 463, 47, 473, 444, 938, 447, 469, 446, 448, 470, 449, 457, 461, 443, 454, 464, 490, 459, 465, 462, 476, 930, 477, 816, 451, 478, 466, 471, 450
1.5–1.99	68, 282, 80, 232, 65, 217, 79, 606, 286, 62, 969, 283, 67, 63, 66, 69, 317, 289, 970, 1403, 73, 302, 219, 74, 1431, 71, 76, 1404, 609, 619, 216, 25, 61, 70, 75, 297, 78, 29, 304, 24, 64, 284, 72, 77, 995, 316, 306, 312, 225, 92, 291, 268, 595, 310, 23, 93, 87, 30, 590, 584	421, 669, 513, 436, 690, 711, 431, 429, 428, 437, 886, 439, 698, 693, 691, 433, 838, 425, 501, 438, 508, 183, 492, 663, 516, 664, 763, 675, 430, 692, 505, 512, 435, 713, 424, 520, 696, 684, 920, 893, 699, 422, 686, 514, 662, 758, 742, 509, 515, 502, 517, 519, 494, 700, 643, 859, 504, 484, 870, 807, 637, 694, 480, 885, 503, 491, 506, 486, 483, 682, 688, 499, 493, 510, 496, 489, 670, 200
1–1.49	301, 27, 22, 26, 21, 97, 100, 86, 88, 31, 40, 89, 94, 91, 83, 99, 309, 38, 605, 35, 95, 320, 34, 84, 265, 36, 644, 39, 305, 98, 37, 82, 85, 783, 33, 32, 852, 90, 81, 315, 214, 614, 206, 314, 224, 585, 596	724, 655, 718, 661, 665, 701, 523, 697, 521, 845, 703, 673, 524, 676, 551, 894, 555, 705, 543, 851, 738, 541, 544, 532, 671, 530, 709, 753, 549, 535, 722, 880, 550, 552, 707, 531, 202, 732, 725, 740, 681, 752, 529, 558, 689, 735, 994, 910, 715, 687, 434, 1159, 727, 817, 683, 432, 631, 423, 685, 695, 1158, 518, 507, 440, 733, 426, 427
0.5–0.99	313, 292, 835, 308, 919, 96, 1471, 856, 307, 1472, 877, 318, 113, 319, 1407, 212, 847, 120, 1440, 108, 1408, 139, 185, 107, 128, 119, 1439, 115, 110, 1104, 112, 911, 135, 279, 848, 114, 118, 133, 794, 140, 102, 127, 109, 827, 105, 134, 1103, 125, 129	180, 154, 178, 161, 779, 363, 373, 162, 177, 176, 533, 377, 175, 174, 173, 729, 172, 757, 163, 170, 1411, 746554, 525, 164, 721, 736, 716, 171, 820, 1459, 739, 766, 165, 813, 168, 376, 545, 169, 380, 548, 167, 1412, 712, 706, 528, 166, 702, 890, 708, 559, 760, 361, 902, 1151, 546, 364, 379, 897, 1460, 1152, 719, 704, 553, 861, 534, 557, 378, 384, 381, 391, 397, 393, 389, 383, 399, 394, 385, 396, 398, 395, 392, 386, 388, 387, 390, 400, 382, 720, 623, 560, 547, 728, 522, 542, 898, 526, 539, 211, 537, 536, 556, 527, 737, 538, 717, 17, 35, 11, 4, 9, 8, 20, 18, 7, 2, 15, 19, 10, 1, 6, 14, 12, 13, 16, 540, 730
0–0.49	121, 136, 138, 610, 116, 592, 130, 784, 104, 566, 799, 106, 117, 101, 126, 122, 896, 826, 983, 137, 131, 123, 111, 132, 984, 124, 878, 945, 831, 563, 103, 932, 37, 1111, 1112	810, 912, 710, 731, 776, 368, 857, 205, 869, 1451, 855, 1435, 1452, 914, 796, 362, 372, 142, 152, 723, 374, 714, 143, 680, 150, 153, 734, 145, 147, 144, 151, 160, 141, 157, 158, 149, 156, 146, 155, 148, 159, 785, 844, 726, 366, 367, 179, 375

The distribution of actuators based on the value of actuation is illustrated in Fig. 7. The figure shows that 22% of the actuated members were lengthened by a value greater than 1.9 mm, while only 15% were shortened with a value larger than 1.9 mm. Furthermore, the percentage of the lengthened and shortened members within 1 to 1.9 mm was 16% and 14%, respectively. In addition, the number of lengthened members within the range of 0.1 mm to 0.99 mm is twice that of shortened.

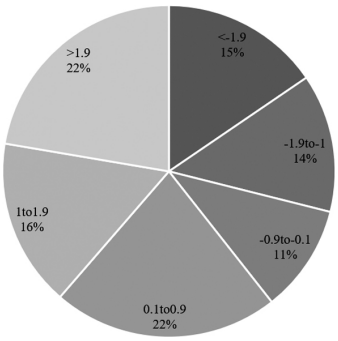

Fig. 7. Distribution of actuators according to the range of actuation

The results presented above were obtained after 21 trials; the 21st trial is considered the optimal solution that accomplishes the task with a minimum number of actuators. Fig. 8 illustrates the step-by-step minimization of the number of actuators in 21 steps. It can be seen that there was a dramatic fall in the number of actuators in the first two steps. Numerically speaking, the actuator numbers declined from 1520 to 1060. In each stage, a set of actuators with negligible actuation were excluded; in step 21, there were no more actuators with less than 0.1 mm thus, the iterations were ended. 0.1 mm is the limit since performing actuation with less than that value is not pragmatic.

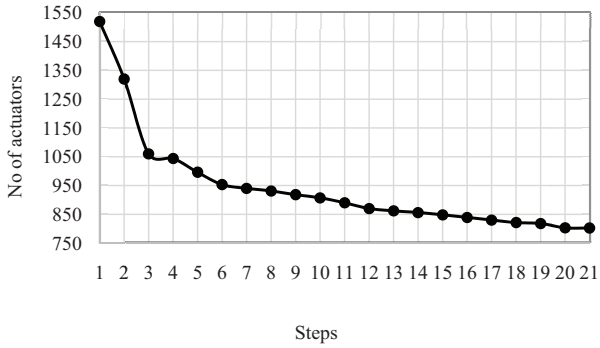

Fig. 8. Minimization of the actuator numbers in twenty-one steps

Figure 9 shows the amount of actuation per step. It can be seen that the maximum amount was recorded in step 3, while the minimum amount was recorded in step 2. However, the actuation value in steps 2, 4, 5, 10, and 11 is less than in step 21; the last step is optimal. The reason is that minimizing the number of actuators is more effective than the amount of actuation. Embedding actuators in the members is more costly than performing the actuation. Nevertheless, comparing the results with the targets is essential; if noticeable dissimilarity exists, the step before will be taken as optimal.

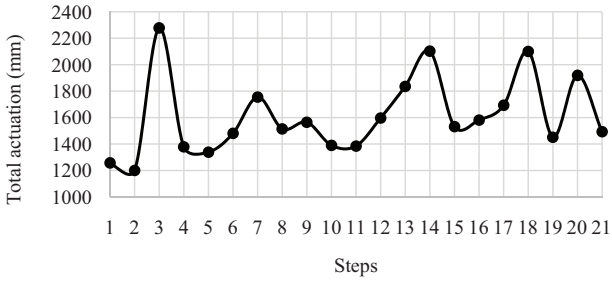

Fig. 9. Optimization in the total actuators in twenty-one iterations

Figure 10 shows the error in percentage between obtained results after adjustment and targets in terms of displacement and stress in 21 steps. In all stages, the dissimilarity was negligible, which confirms that the technique works very well.

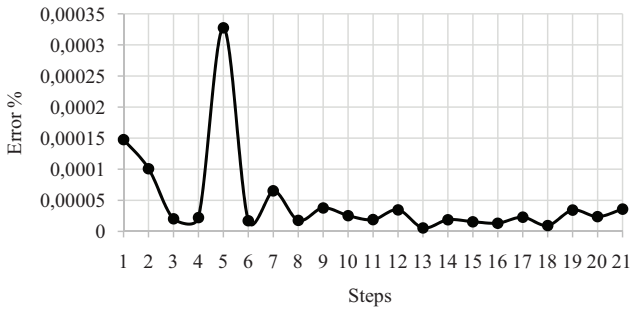

Fig. 10. The dissimilarities between the outcomes and the goals in twenty-one iterations

4. Conclusions

In this paper, the disturbed shape of the outer face of a numerical model of a double-layer spherical structure under vertical loading has been reshaped. Meanwhile, the axial forces of members were observed while optimization techniques were implemented to use as few actuators as possible.

- The displacement in the X,Y and Z directions of the outer layer joints of the double layer model was nullified.
- The stress on members is kept within the elastic range.
- The optimum actuation set was obtained after 21 iterations.
- It was planned to exclude actuators with less than 0.1 mm, since it is not implemanted in practice.
- The adjustment has been made with the optimum actuation of 1493 mm.
- Number of actuators minimized to 802.
- 39% of actuated members were shortened, while 61% were lengthened.

– The compression force was dominant after adjustment.
– SAP2000 program was used to analyze the structure before and post-adjustment in line with MATLAB to see if the results matched.
– The dissimilarity between the targets and the results was negligible.

References

[1] X. Chang, X. Haiyan, "Using sphere parameters to detect construction quality of spherical buildings", in *2nd International Conference on Advanced Computer Control*. IEEE, 2010; DOI: 10.1109/ICACC.2010.5487073.

[2] B. Richard, "Las Vegas: past, present and future", *Journal of Tourism Futures*, 2018, vol. 4, no. 3, pp. 182–192; DOI: 10.1108/JTF-05-2018-0027.

[3] N.M. Saeed, A.S.K. Kwan, "Simultaneous displacement and internal force prescription in shape control of pin-jointed assemblies", *AIAA Journal*, 2016, vol. 54, no. 8, pp. 2499–2506; DOI: 10.2514/1.J054811.

[4] C.J. Weeks, "Static shape determination and control of large space structures: I. The flexible beam", *Journal of Dynamic Systems, Measurement and Control*, 1984,vol. 106, no. 4, pp. 261–266; DOI: 10.1115/1.3140683.

[5] R.T. Haftka, H.M. Adelman, "An analytical investigation of shape control of large space structures by applied temperatures", *AIAA Journal*, 1985, vol. 23, no. 3, pp. 450–457; DOI: 10.2514/3.8934.

[6] H. Irschik, "A review on static and dynamic shape control of structures by piezoelectric actuation", *Engineering Structures*, 2002, vol. 24, no. 1, pp. 5–11; DOI: 10.1016/S0141-0296(01)00081-5.

[7] R.T. Haftka, "Limits on static shape control for space structures", *AIAA Journal*, 1991, vol. 29, no. 11, pp. 1945–1950; DOI: 10.2514/3.10823.

[8] H. Pichler, J. Irschik, "Dynamic shape control of solids and structures by thermal expansion strains", *Journal of Thermal Stresses*, 2001, vol. 24, no. 6, pp. 565–576; DOI: 10.1080/014957301300158102.

[9] Z. You, "Displacement control of prestressed structures", *Computer Methods in Applied Mechanics and Engineering*, 1997, vol. 144, no. 1-2, pp. 51–59; DOI: 10.1016/S0045-7825(96)01164-4.

[10] S.-M. Yang, J.-H. Roh, J.-H. Han, I. Lee, "Experimental studies on active shape control of composite structures using SMA actuators", *Journal of Intelligent Material Systems and Structures*, 2006, vol. 17, no. 8-9, pp. 767–777; DOI: 10.1177/1045389X06055830.

[11] Z. Wang, T. Li, Y. Cao, "Active shape adjustment of cable net structures with PZT actuators", *Aerospace Science Technology*, 2013, vol. 26, no. 1, pp. 160–168; DOI: 10.1016/j.ast.2012.03.001.

[12] K. Wang, A. Preumont, "Shape control of an adaptive spherical shell reflector under space environment", in *Eighth Symposium on Novel Photoelectronic Detection Technology and Applications*, vol. 12169. SPIE, 2022, pp. 2462–2467; DOI: 10.1117/12.2625829.

[13] J. Du, Y. Zong, H. Bao, "Shape adjustment of cable mesh antennas using sequential quadratic progra mming", *Aerospace Science and Technology*, 2013, vol. 30, no. 1, pp. 26–32; DOI: 10.1016/j.ast.2013.06.002.

[14] J. Du, H. Bao, C. Cui, "Shape adjustment of cable mesh reflector antennas considering modeling uncertainties", *Acta Astronautica*, 2014, vol. 97, pp. 164–171; DOI: 10.1016/j.actaastro.2014.01.001.

[15] A.M. Sharabash, B.O. Andrawes, "Application of shape memory alloy dampers in the seismic control of cable-stayed bridges", *Engineering Structures*, 2009, vol. 31, no. 2, pp. 607–616; DOI: 10.1016/j.engstruct.2008.11.007.

[16] A.S.K. Kwan, S. Pellegrino, "Prestressing a space structure", *AIAA Journal*, 1993, vol. 31, no. 10, pp. 1961–1963; DOI: 10.2514/3.11876.

[17] N.M. Saeed, A.A.H. Manguri, A.M. Adabar, "Shape and force control of cable structures with minimal actuators and actuation", *International Journal of Space Structures*, 2021, vol. 36, no. 3, pp. 241–248; DOI: 10.1177/09560599211045851.

[18] S. Krishnan, "Structural design and behavior of prestressed cable domes", *Engineering Structures*, 2020, vol. 209, art. ID 110294; DOI: 10.1016/j.engstruct.2020.110294.

[19] Y. Xue, Y. Luo, X. Xu, H.-P. Wan, Y. Shen, "A robust method for pre-stress adjustment of cable-strut structures based on sparse regression", *Engineering Structures*, 2021, vol. 246, art. ID 112987; DOI: 10.1016/j.engstruct.2021.112987.

[20] A.A. Manguri, A.S.K. Kwan, N.M. Saeed, "Adjustment for shape restoration and force control of cable arch stayed bridges", *International Journal of Computational Methods and Experimental Measurements*, 2017, vol. 5, no. 4, pp. 514–521; DOI: 10.2495/CMEM-V5-N4-514-521.

[21] W. Chen, D. Wang, M. Li, "Static shape control employing displacement–stress dual criteria", *Smart Materials and Structures*, 2004, vol. 13, no. 3, pp. 468–472; DOI: 10.1088/0964-1726/13/3/003.

[22] J.J. Joo, B. Sanders, T. Johnson, M.I. Frecker, "Optimal actuator location within a morphing wing scissor mechanism configuration", in *Smart Structures and Materials 2006: Modeling, Signal Processing, and Control*, vol. 6166. SPIE, 2006, pp. 24–35; DOI: 10.1117/12.658830.

[23] A. Sabouni-Zawadzka, A. Zawadzki, "Simulation of a deployable tensegrity column based on the finite element modeling and multibody dynamics simultions", *Archives of Civil Engineering*, 2020, vol. 66, no. 4, pp. 543–560; DOI: 10.24425/ace.2020.135236.

[24] J. Nocedal, S. Wright, *Numerical optimization*. New York , USA: Springer Science & Business Media, 2006.

[25] L.Y. Shen, G.Q. Li, Y.F. Luo, "Displacement control of prestressed cable structures (in Chinese)", *Journal of Tongji University Natural Science*, 2006, vol. 34, no. 3, pp. 291–295.

[26] X. Xu, Y.Z. Luo, "Multi-objective shape control of prestressed structures with genetic algorithms", *Proceedings of the Institution of Mechanical Engineers, Part G: Journal of Aerospace Engineering*, 2008, vol. 222, no. 8, pp. 1139–1147; DOI: 10.1243/09544100JAERO394.

[27] X. Xu, Y.Z. Luo, "Non-linear displacement control of prestressed cable structures", *Proceedings of the Institution of Mechanical Engineers, Part G: Journal of Aerospace Engineering*, 2009, vol. 223, no. 7, pp. 1001–1007; DOI: 10.1243/09544100JAERO455.

[28] G. Senatore, A.P. Reksowardojo, "Force and Shape Control Strategies for Minimum Energy Adaptive Structures", *Frontiers in Built Environment*, 2020, vol. 6, art. ID 105; DOI: 10.3389/fbuil.2020.00105.

[29] M. Liu, Q. Sun, H. Yu, J. Yang, T. Zhang, "Static and dynamic test analysis of a 12-years old 14 000-ton cable-stayed bridge used swivel construction technology", *Archives of Civil Engineering*, 2021, vol. 67, no. 4, pp. 369–381; DOI: 10.24425/ace.2021.138505.

[30] E.G. Christoforou, A. Müller, M.C. Phocas, M. Matheou, S. Arnos, "Design and control concept for reconfigurable architecture", *Journal of Mechanical Design*, 2015, vol. 137, no. 4, art. ID 042302; DOI: 10.1115/1.4029617.

[31] N. Saeed, A. Manguri, S. Abdulkarim, A. Shekha, "Shape Restoration of Deformed Egg-Shaped Single Layer Space Frames", in *2019 International Conference on Advanced Science and Engineering (ICOASE), Duhok, Kurdistan Region, Iraq*. IEEE, 2019, pp. 220–225; DOI: 10.1109/ICOASE.2019.8723714.

[32] A. Manguri, N. Saeed, B. Haydar, "Optimal Shape Refurbishment of Distorted Dome Structure with Safeguarding of Member Stress", in *7th International Engineering Conference "Research & Innovation amid Global Pandemic"(IEC2021), Erbil, Iraq*. IEEE, 2021, pp. 90–95; DOI: 10.1109/IEC52205.2021.9476107.

[33] N. Saeed, A. Manguri, S. Al-Zahawi, "Optimum Geometry and Stress Control of Deformed Double Layer Dome for Gravity and Lateral Loads", in *7th International Engineering Conference "Research & Innovation amid Global Pandemic"(IEC2021), Erbil, Iraq*. IEEE, 2021, pp. 84–89; DOI: 10.1109/IEC52205.2021.9476094.

[34] S. Patnaik, "The integrated force method versus the standard force method", *Computers and Structures*, 1986, vol. 22, no. 2, pp. 151–163; DOI: 10.1016/0045-7949(86)90061-1.

[35] J.-O. Sperle, K. Olsson, "High strength and ultra high strength steels for weight reduction in structural and safety-related applications", in *29 th International Symposium on Automotive Technology and Automation*, vol. 1, 1996, pp. 115–125.

[36] MATLAB, "Constrained Nonlinear Optimization Algorithms", Mathworks. [Online]. Available: https://www.mathworks.com/help/optim/ug/constrained-nonlinear-optimization-algorithms.html. [Accessed: 12 Mar 2022].

Received: 2022-06-21, Revised: 2022-08-08